

Paper No. **890314**

Published in NRC-TRB  
Transportation Research Record No.  
1278, "Dynamic Testing of  
Aggregates and Soils and Lateral  
Stress Measurement." 1990.

# PREPRINT

**Title:\_\_\_\_\_ Field Experience with the \_\_\_\_\_**  
**\_\_\_\_\_ Back-Pressured Ko \_\_\_\_\_**  
**\_\_\_\_\_ Stepped Blade \_\_\_\_\_**

**Author(s):\_\_\_\_\_**  
**\_\_\_\_\_ R. L. Handy, Chris Mings, David Retz, \_\_\_\_\_**  
**\_\_\_\_\_ and Donald Eichner \_\_\_\_\_**

Transportation Research Board  
69th Annual Meeting  
January 7-11, 1990  
Washington, D.C.

FIELD EXPERIENCE WITH THE BACK-PRESSURED  $K_0$  STEPPED BLADE

by Richard L. Handy<sup>1</sup>, Chris Mings<sup>2</sup>, David Retz<sup>3</sup>,  
and Donald Eichner<sup>4</sup>

Specialty Session on Measurement of Lateral Soil Stress  
The 69th Annual Meeting of the Transportation Research Board

January, 1990

Spangler Geotechnical Laboratory  
Department of Civil and Construction Engineering  
Iowa State University  
Ames, Iowa, 50011

---

<sup>1</sup> Anson Marston Distinguished Professor of Engineering, Department of Civil and Construction Engineering, Iowa State University, Ames, Iowa, 50011; Ph. 515-294-7690.

<sup>2</sup> Engineer, Geo-Hydro Engineers, Inc., 100 E. Callahan St., Rome, Ga., 30161; Ph. 404-234-0696.

<sup>3</sup> Engineer, Burns & McDonald Engineering, 4600 E. 63d St., Kansas City, Mo., 64141; Ph. 816-333-4375

<sup>4</sup> Adjunct Assistant Professor of Industrial Engineering, Iowa State University, Ames, Iowa, 50011; Ph. 515-294-6518.

## Abstract

The  $K_0$  Stepped Blade measures soil pressures developed from penetration of soil by progressively thicker steps of a thin blade. The pressures then are extrapolated to obtain an hypothetical pressure acting on a zero-thickness blade. In many instances measures of lateral subgrade modulus and limit pressure also may be obtained. The Stepped Blade Test or SBT falls between the conventional pressuremeter and the Dilatometer in speed and ease of operation, faster than the pressuremeter and slower than the Dilatometer.

Pneumatic pressure cells give 1:1 calibrations and ease of field repair. An improved back-pressured readout system simultaneously pressurizes two cell areas at slightly different pressures, the two areas being sealed one from the other by soil pressure acting against a cover membrane; when the internal gas pressure equals the external soil pressure, the seal is broken and gas flows within the cell causing the differential pressure to drop to zero. This signals when the main gauge pressure should be read. The system then is vented and switched to the next cell for the next reading. Readings are reproducible to the nearest gauge dial increment, which is 1 psi (7 kPa).

Field test data and discussions are presented to show some applications for lateral soil stress data obtained with the  $K_0$  Stepped Blade: Most applications involve defining recent stress history, including consolidation, compaction, and influence from pile and retaining walls, from the relation between the measured lateral in situ stress and depth. Demonstrations include deter-

mining the soil consolidation state and the preconsolidation pressure and/or effective depth of overburden removal; the existence of clay expansion pressure; or the presence of passive pressure indicative of imminent bearing capacity failure; and the effects of deep dynamic compaction and of pile driving.

Tests cannot be performed in stony soils due to difficulty in pushing the blade and the risk of damaging the pressure cells; nor can lateral stresses be measured in very soft clays where pressures from insertion of the blade exceed the limit pressure, probably attributable to the development of excess pore water pressure.

## INTRODUCTION

Principle.  $K_0$  Stepped Blade was developed to measure lateral soil pressures in situ. The blade is rectangular in shape, sharpened on the lower end, and becomes progressively thicker up the shank in a series of flat rectangular steps, Fig. 1. Each step has its own pressure cell that measures the lateral soil pressure exerted on that step after the blade has been pushed into the soil. Tests are performed by drilling to above the test depth and alternately pushing one step length and reading all embedded pressure cells. Thus a series of pressure readings is obtained at each sub-depth. By plotting the several step pressures measured at each sub-depth as a function of the step thickness, an extrapolation may be made as shown in Fig. 1 to give hypothetical pressures on a zero thickness blade, as an indication of the lateral total stress existing in the soil prior to insertion of the blade. Effective stresses are estimated by subtracting static pore pressures calculated from depth below a water table or measured with piezometers.

History. The Stepped Blade was developed for the U.S. Federal Highway Administration to provide an alternative means for measuring lateral in situ stress in soil. The goal was a method that would be accurate to within 1 lb/in.<sup>2</sup> (7 kPa), and more rapid and more readily performed than self-boring pressure-meter tests. The approach was borrowed from analytical chemistry--to recognize that some disturbance to the soil is inevitable if a hole is bored or an instrument inserted, so instead of attempting to prevent disturbance it is allowed to happen, and

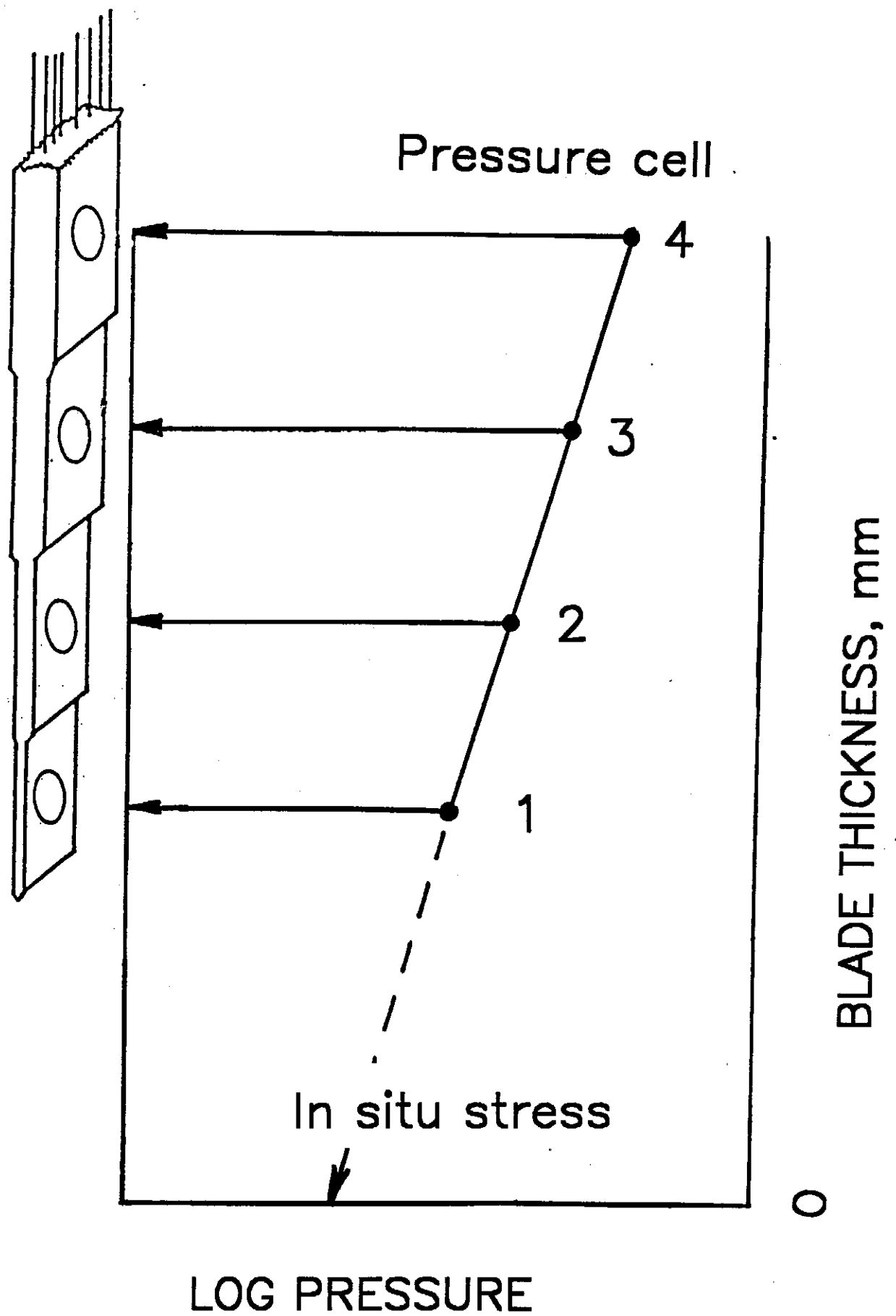


Fig. 1. Principle of the Ko Stepped Blade Test (SBT).

its effects removed by extrapolation.

The initial development of the Stepped Blade was made during 1976-81 by Soil Systems, Inc., Marietta, Ga., with Iowa State University as subcontractor. Tests and developments were continued at Iowa State under FHWA sponsorship during 1982-87, with Eichner Engineering Co. as subcontractor for developmental work, and J.-L. Briaud's group at Texas A&M University doing the comparative pressuremeter and finite element studies. During this time the Blade went through five major redesigns, the latest being to incorporate a back-pressure readout system, and a back rib to stiffen and strengthen the blade without appreciably affecting pressure readings.

The Blade development was preceded and was partly inspired by the pioneering work of Marchetti with the Dilatometer. The main differences between the SBT and the Dilatometer are: The Blade has several steps, each with its own pressure cell, and is much thinner than the Dilatometer. The Blade cells are pneumatic and non-expansive, the Dilatometer electro-pneumatic and expansive. The Dilatometer is shorter and more rugged and can be pushed continuously, whereas the blade requires pre-drilling to each test depth where it then is pushed. The soil responses differ, as do the methods for data interpretation. The Dilatometer has a longer history of use.

#### DEVICE

w/t ratio. Most in situ soil testing devices are cylindrical in shape, with the lower end sharpened to a cone or hollow cone. An obvious difference between pushing a thin, flat blade

and pushing or driving a cone is to reduce the amount of soil displacement and disturbance; furthermore the thinner the blade, the less should be the disturbance.

Laboratory tests with layered modeling clay showed a linear relationship between the thickness of the disturbed zone and the thickness of the blades, the blade width being constant (1). The ratio of width to thickness can be used as a dimensionless measure of relative blade thinness; the higher the ratio, the thinner the blade. In the case of solid cylindrical or conical test devices the ratio is 1.0. Ratios for these and other devices including the current SBT are listed in Table 1 and shown graphically in Fig. 2. In the case of the two samplers listed, the width is taken as the inside circumference of the sampler, the  $t$  is twice the wall thickness, since soil is displaced only towards the outside.

-----  
Table 1. Width:thickness ratios for some soil penetration test and sampling devices.

<u>Device</u>	<u>t, mm</u>	<u>w, mm</u>	<u>w/t</u>
Standard cone	35.7	35.7	1.0
SPT	15.9	110	6.9*
3-in. Shelby tube	3.3	229	69.4*
NX vane	3.2	25.4	8.0
Dilatometer	14	95	6.8
Glottl cell	5	100	20.0
SBT step 1	3	63.5	21.2
step 2	4.5	63.5	14.1
step 3	6	63.5	10.6
step 4	7.5	63.5	8.5

\*  $t$  is 2X the wall thickness and  $w$  is the inside circumference since the soil is presumed to be displaced only to the outside.



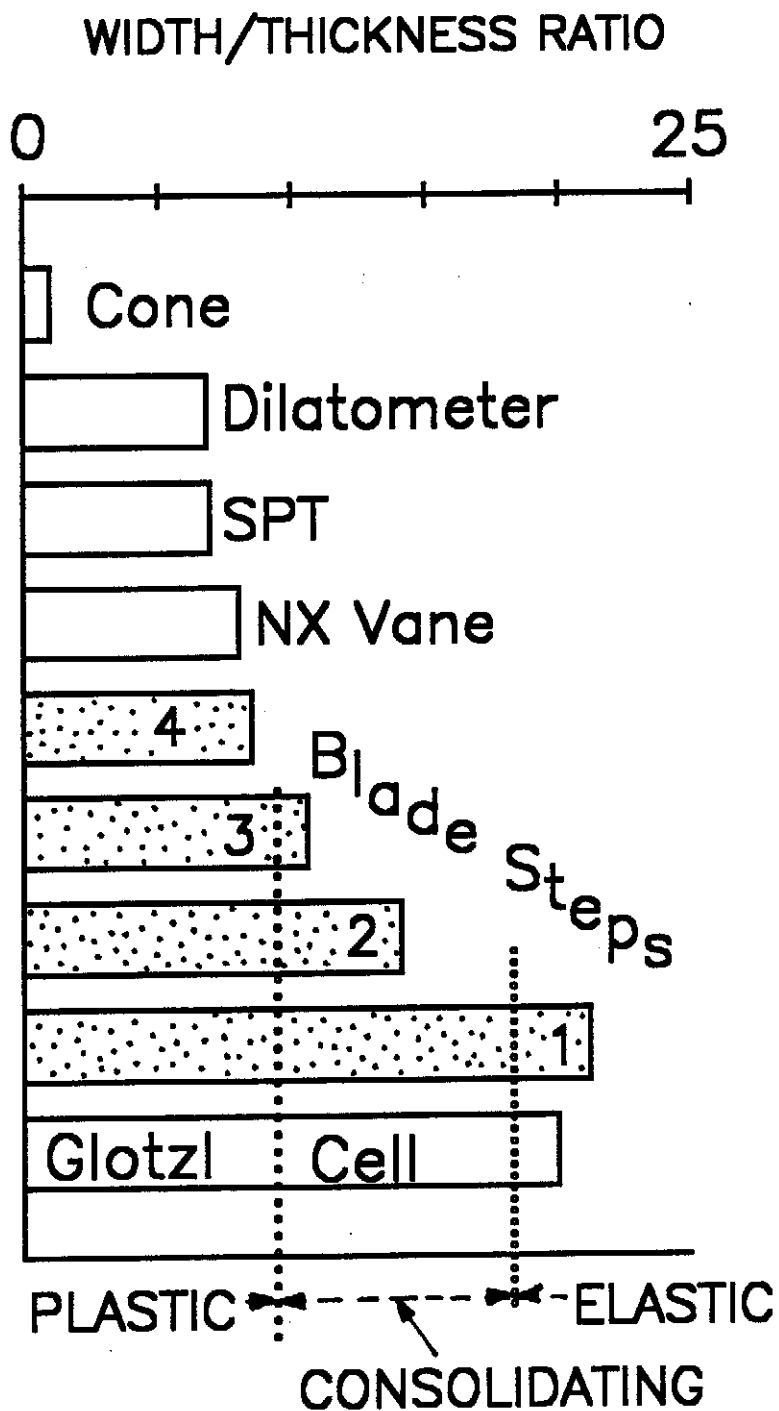


Fig. 2. Width:thickness ratios for some soil penetrating devices, and dominating behavior as inferred from Stepped Blade tests.

Back-pressured pneumatic pressure cells. A late development in the blade research, and a key factor for improving the reliability and precision of the pressure readings, was the invention of a back-pressured system for operating and reading the pneumatic pressure cells (2). Most pneumatic cells, including those of earlier model blades, operate by applying inside gas pressure against a diaphragm exposed to the pressure to be measured; then when the pressures are equalized, the diaphragm lifts sufficiently to allow gas to flow through the cell and be detected with a flowmeter. These are referred to as normally closed or venting type cells (3, par. 8.3). In early versions of the blade, pressure was applied to area A shown in Fig. 3, and area B was monitored for flow. After flow is achieved, gas pressures may be reduced to obtain a pressure reading for the initiation of a no-flow condition, but to save time and prevent cycling of the soil displacement this was not done in the blade tests. Difficulties were experienced from the diaphragms either leaking or sticking, and from the difficulty of monitoring for changes in gas flow through long pressure lines. In some instances individual blade cells had calibration factors that not only were different for each cell, but tended to change (4). A strain-gauge cell that directly measures effective stress was developed (5) but was not sufficiently reliable for field use, so emphasis returned to the pneumatic cell.

Laboratory tests indicated that sticking was more likely to occur at high pressures, and also was quite sensitive to minor changes in the height of the threshold C in Fig. 3. As only part

# Back-Pressured Pneumatic Cell

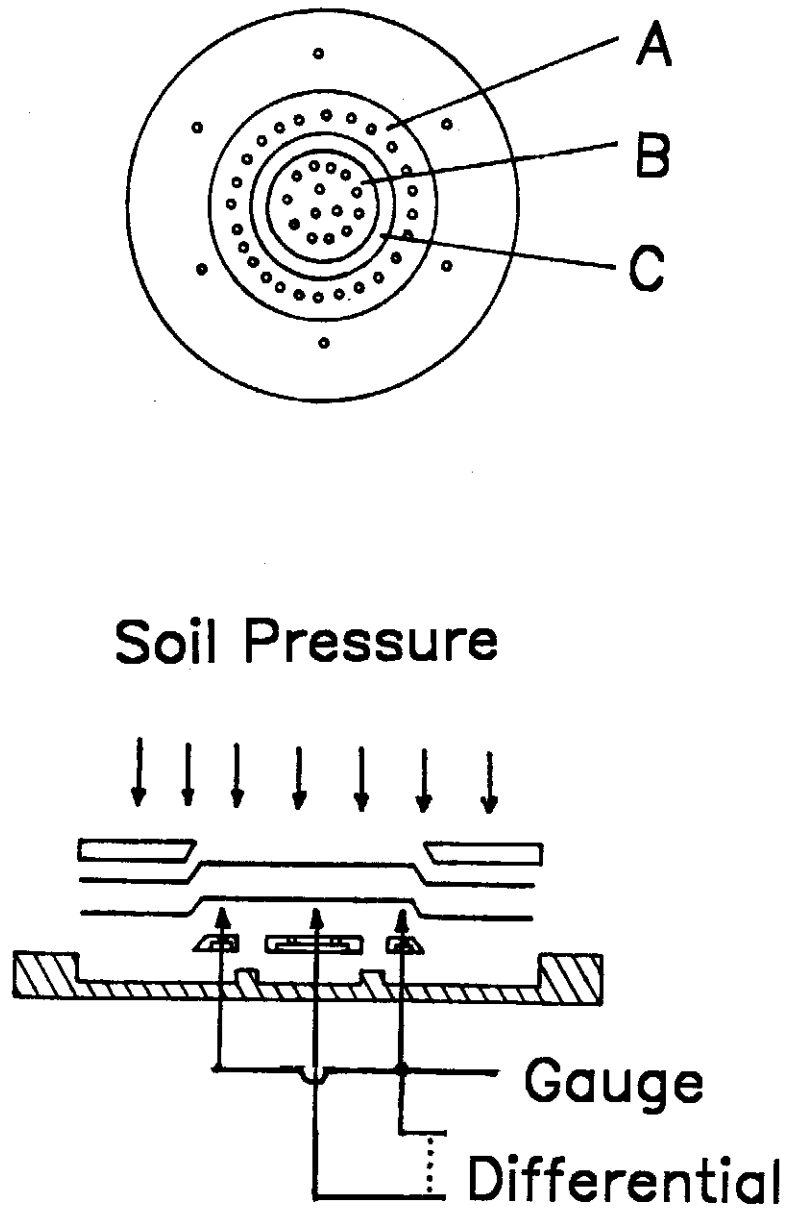


Fig. 3. Components of the pneumatic pressure cell (not to scale).

of the backside of the diaphragm was pressurized, which seemed a rather inefficient and possibly error-prone way to balance the soil pressure, a scheme was devised to simultaneously pressurize both areas A and B, while maintaining a small differential pressure between the two areas. As the two pressures are raised, when the higher of the two pressures reaches the soil pressure the membrane lifts sufficiently to allow a small amount of gas flow within the cell, reducing the differential pressure to near zero and usually causing a perceptible pause in the rate of increase of the main gauge pressure. The loss of differential pressure tells the technician when to read the pressure gauge, and the serendipitous pause in climb of the main gauge needle makes it easier to read.

The method used for simultaneous pressurization is quite simple, shown diagrammatically in Fig. 4. A needle valve T1 controls the rate of pressure increase, and ordinarily is set for a rate of increase of about 1 psi/s (7kPa/s). Nitrogen, compressed air, or carbon dioxide regulated to a maximum pressure of 300 psi (2000 kPa) is used as a gas source. The second needle valve T2 is left closed until both gauges approach 8 to 10 psi (60 to 80 kPa), when it is opened slightly and adjusted to give a differential pressure that will tend to remain constant without further adjustment. As the soil pressure is approached, some leakage and reduction of differential pressure may occur, particularly if the soil pressure is unevenly distributed around the cell threshold C in Fig. 3, in which case T2 may be partially shut to sustain  $\Delta P$  until a sharp drop occurs. It will be seen that if the diaphragm is lifted,  $\Delta P$  must go to near zero regard-

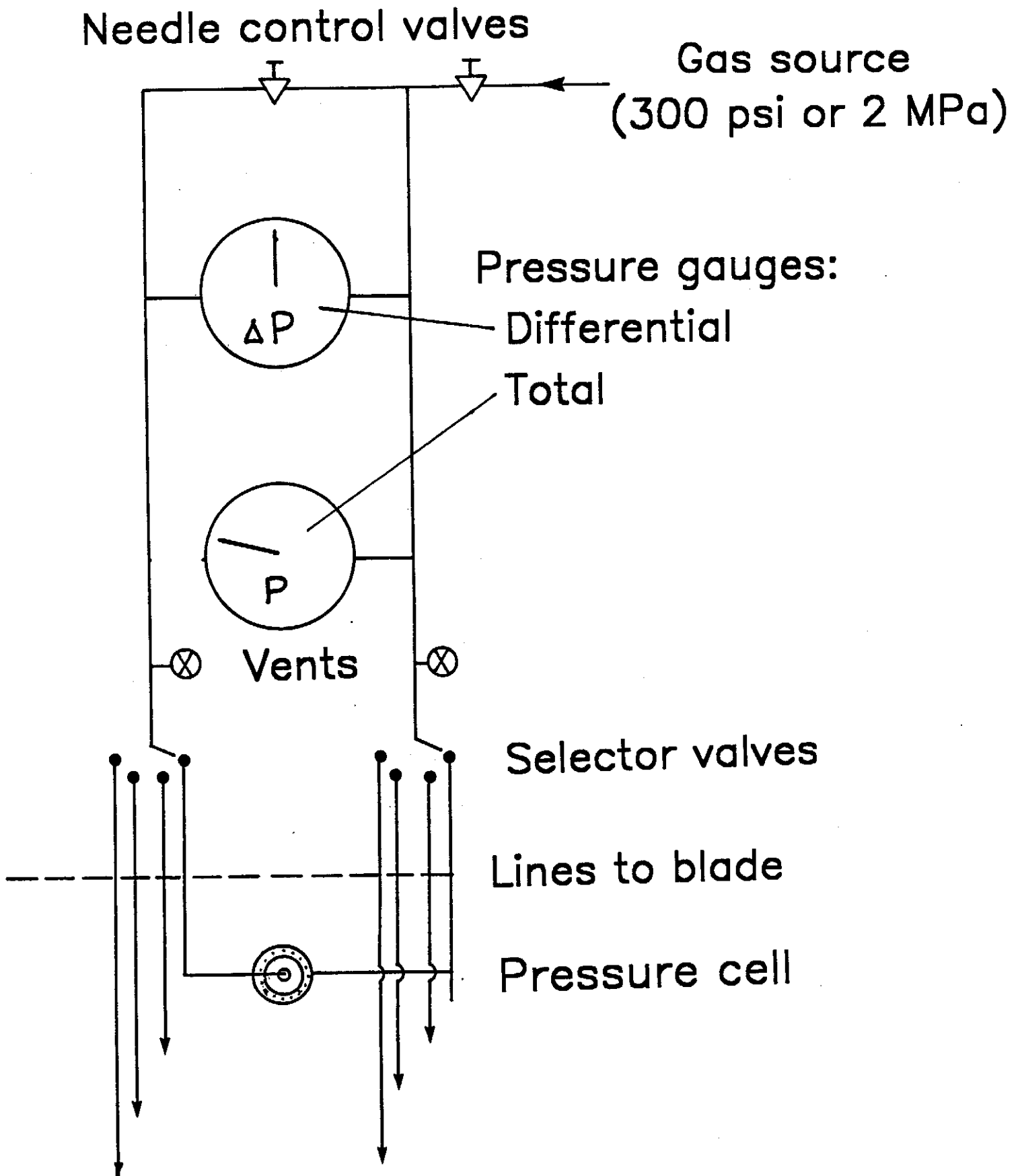


Fig. 4. Schematic diagram of the back-pressured blade console.

less of the position of T2.

#### SOIL RESPONSES

Consolidation response. It was anticipated and then shown by laboratory experiments that the thicker the blade step, the higher the pressure induced by insertion of that step into the soil (1). An empirical relationship was defined between thickness and log pressure, as shown in Fig. 5(a). Regression of the data typically will give  $r^2$  values in the range 0.97-1.0. The semilogarithmic response corresponds to a linear relation of void ratio to log pressure, and on this basis is assumed to be indicative that pressures mainly reflect a consolidating behavior of the soil next to the blade. Consolidation may be aided by the relative thinness of the blade compared with other devices, and a zone of reduced stress and low or negative pore pressures extending out from both edges of the blade after insertion. Since consolidation may be far from complete when blade cell pressures are read, the sequence of readings is such that approximately the same amount of time lapses between insertion and reading of each pressure cell. Variable times from a few minutes to two weeks have been used in some soils without affecting the extrapolated soil pressures.

Elastic response. Field use of the SBT indicated that the soil response might not always be so simple as initially envisioned because the pressure sometimes is higher on the first, thinnest blade step than on the subsequent thicker steps. This behavior is shown in Fig. 5(b), where it is followed by the more usual behavior. The high-first-point behavior did not occur in

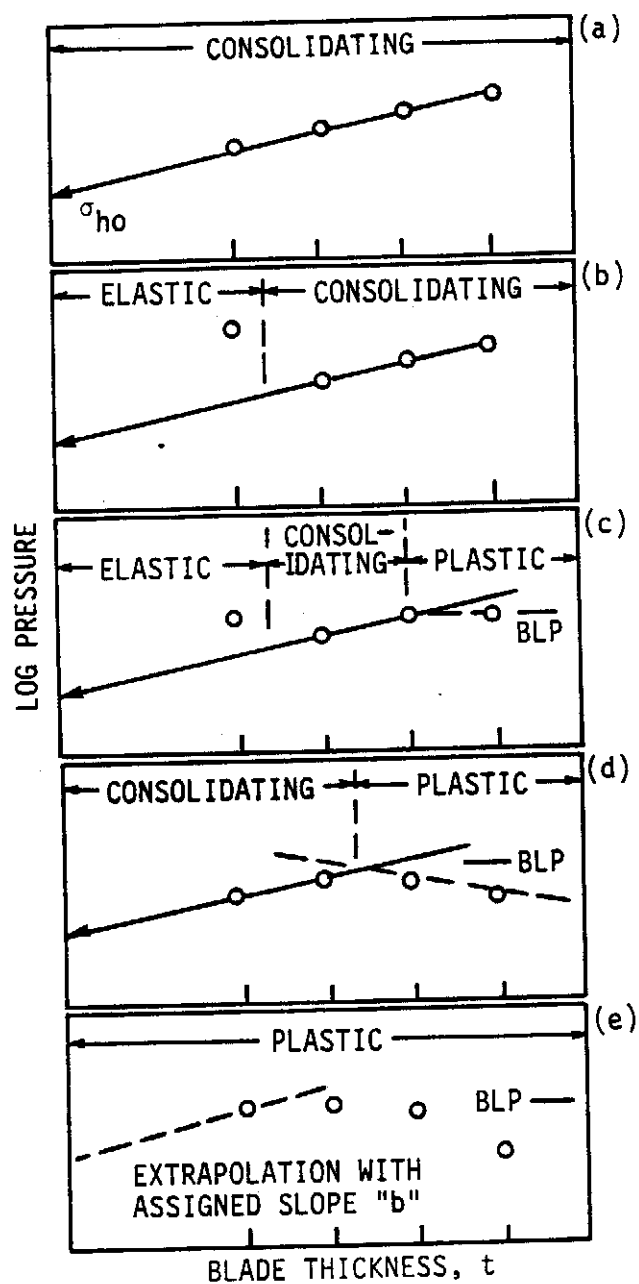


Fig. 5. Selected data plots of log blade pressure as a function of blade thickness  $t$ , and inferred soil response. BLP = blade limit pressure.

the laboratory developmental tests performed on remolded samples.(1)

The high first-point behavior, which at first was thought to be anomalous, was most commonly observed in stiff clay loam soils such as glacial till, and in lightly cemented silts and sands. It therefore is believed to reflect a relict soil structure that is left intact by penetration of the thinnest blade step and breaks down during penetration of the next thicker blade step. In this connection, it should be noted that the blade imposes constant deflection instead of constant stress conditions as in the conventional consolidation test; thus, as illustrated in Fig. 6, a stress relief from B on the elastic response curve to C and D on the virgin compression curve should be possible if the soil structure breaks down. An analogous reduction does not occur in conventional constant-stress consolidation tests because the path goes from C downward to E. The discontinuity in soil behavior suggests separation of the data into two stress regimes.

If this interpretation is correct, the pressure on the first step should be essentially an elastic response that may be used to compute a lateral subgrade modulus. In support of this, it was found that correlations between first-step pressures and the pressuremeter moduli were substantially better than were obtained by subtracting consecutive step pressures.(6) .

In no case was the elastic response observed on other than the first blade step, indicating that a w/t ratio that is less than 14 must break down the soil structure. A value of 18 was arbitrarily selected to define an approximate elastic range shown



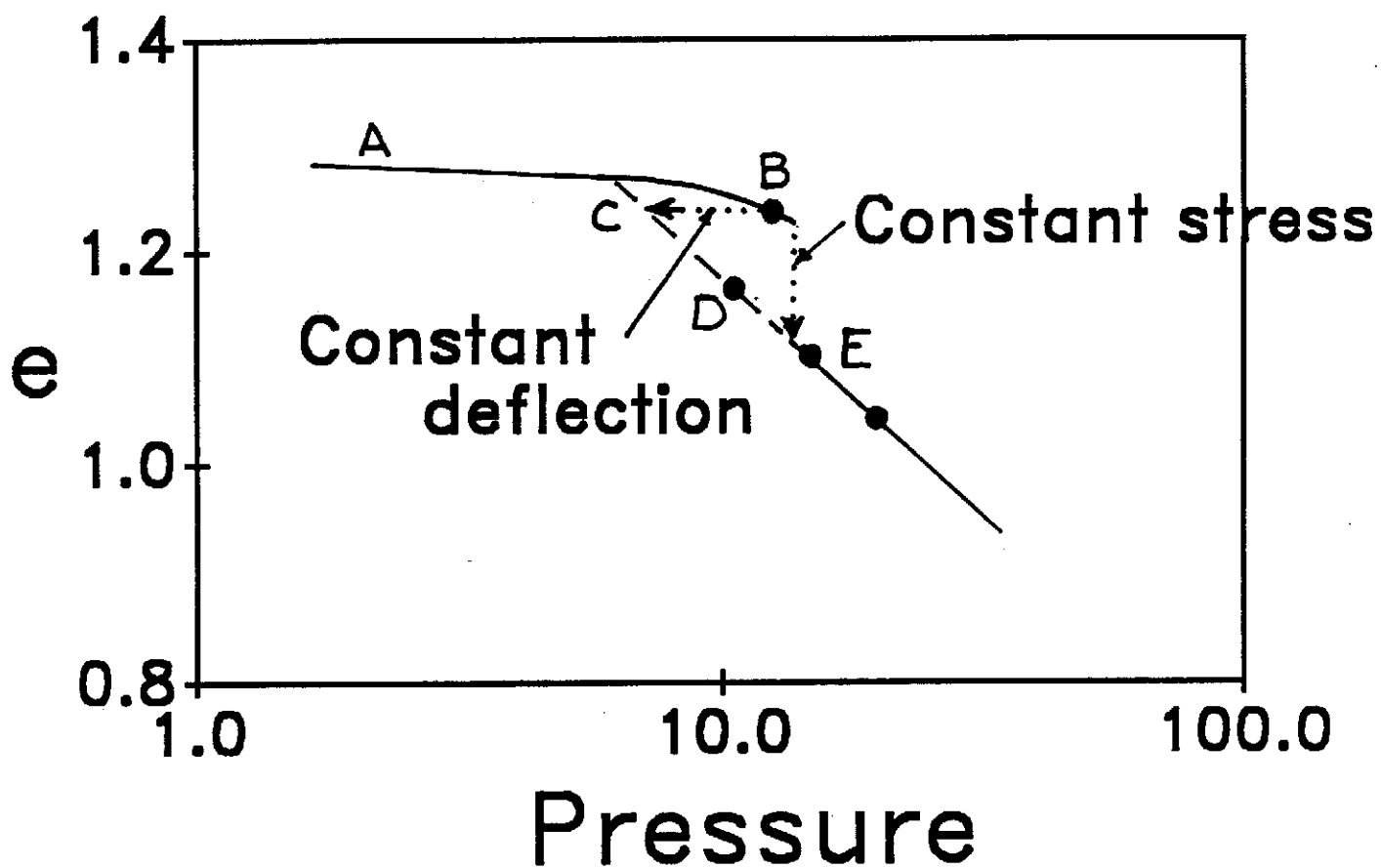


Fig. 6. Hypothetical  $e$ -log  $p$  diagram of a slightly cemented soil to show how a high first point may develop in Stepped Blade tests: Collapse of the soil structure relieves the stress from B to C and D on the virgin compression curve.

in Fig. 2.

Plastic failure. A second, more common, departure from a semilogarithmic relationship between soil pressure and blade thickness was previously described and attributed to a limit pressure--that is, relief of the consolidating pressure by plastic failure wherein the dominating behavior is one of being pushed aside instead of being compressed (1). This is suggested when there is a constant or decreasing blade pressure with increasing step thickness, as shown to the right in Fig. 5(c, d, and e). The phenomenon is most common in soft, saturated clay soils where it undoubtedly reflects the development of excess pore pressure. Supporting this interpretation is that the blade limit pressure has been shown to correlate with the pressuremeter limit pressure (6), and soil pressures measured in soft clays with the relatively thick Dilatometer have been shown to be mainly excess pore water pressures (7). Best would be to determine effective stress and pore water pressure, and to this end a pore pressure port has been incorporated into the thickest step of the blade but has not been subjected to field tests as yet. The limit pressure response usually occurs by the fourth step, and in soft soils may also occur upon insertion of thinner steps--in some instances, as shown in Fig. 5(e), preventing a meaningful extrapolation to obtain a lateral in situ stress.

Because plastic failure often occurs with insertion of the fourth blade step, the consolidating response mechanism appears normally to be limited to w/t ratios that are less than 8.5, which is the value shown in Fig. 2. However, it should be emphasized that plastic failure is not inevitable with the fourth

step, and the limiting w/t ratios will vary with the individual soil and moisture condition.

Implications. Although at first put in the category of a nuisance, the different modes of soil behavior suggested in this analysis can give additional information relative to the soil being tested, and also may give important insights into other in situ test methods. For example, it would appear from the information in Fig. 2 that the pushing of cones--whether Dutch, piezo, expandable, or ice cream--can be expected to cause plastic failure that is sufficient to modify previously existing lateral stresses and bring them to a limit pressure. On the basis of their w/t ratios, the same interpretation may be applied to the SPT and Dilatometer, which can be advantageous by removing the influence of variable  $K_0$  and allowing a focus on other material properties. Where the stepped blade and Dilatometer have been used in the same soil,  $P_o$  pressures measured with the Dilatometer are approximately the same as pressures measured by the thickest section of the stepped blade, both blades having similar w/t ratios and appearing to induce limit pressure responses. This also means that sleeve friction on a cylindrical probe probably is not a valid measure of the lateral stress and  $K_0$  that existed prior to insertion of the test device. The elastic modulus obtained with the Dilatometer derives from the pressure to bulge out its central diaphragm, which probably does not reinitiate plastic failure; however, this also implies that the modulus measured by the Dilatometer is buffered by an intermediate zone that has undergone plastic failure and supports the need for

empirical correlations.

Also in Fig. 2 will be seen that the only devices that appear to be thin enough to be pushed into soil without inevitably collapsing its structure are the Glotzl cell and the first step of the Stepped Blade. The maximum elastic response pressure that can be measured by the Blade also should represent a real or apparent lateral preconsolidation pressure as influenced by cementation, aging stress history, etc., since pressures in excess of this amount will break down the soil structure and cause the soil to enter a consolidating stage, a matter that was first discovered by Lutenecker (7).

The blade appears unique among in-situ test instruments in showing an identifiable consolidating behavior; for example, the pressuremeter, expanding in a pre-bored hole, is interpreted as causing elastic response with direct transition into plastic shear, perhaps related to the relatively poor drainage in this test.

It is important in the interpretation of blade data to recognize possible changes in response mechanisms to avoid error. For example, data points that are low because of attaining a limit pressure will tilt the slope of the graph and give too high an extrapolated in situ stress. A flow path that attempts to remove subjectivity in interpreting the data is presented in Appendix A.

Representative data. Representative data plots from tests in a hydraulic fill sand near San Francisco and a loessial silt in western Nebraska are shown in Fig. 7. Test data from a soft alluvial clay in Nebraska, a medium stiff clay in Houston, and a

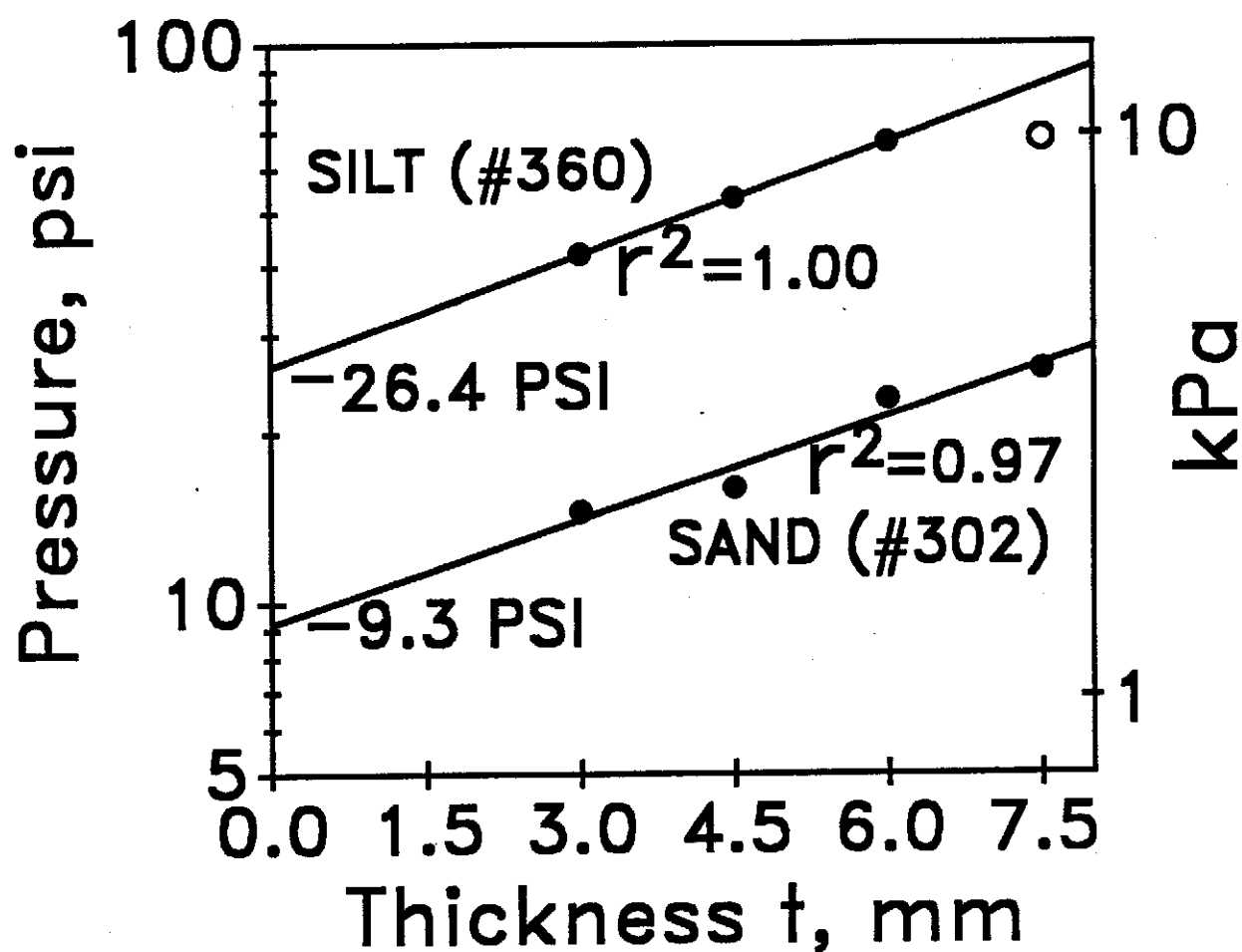


Fig. 7. Representative test data for an unsaturated loessial silt and for a saturated sand. Open point was not included in the regression. Test numbers refer to ref. (6).

very stiff clay near College Station, Texas, are shown in Fig. 8. To reduce subjectivity in selecting the data to be shown, all are for tests at approximately the same depth which was arbitrary selected to be 15 ft (5 m), and only the uppermost, 4-point data sets are shown. (Additionally a 3-point, a 2-point, and a 1-point set is obtained at each testing sub-depth and is subjected to the same methods for data interpretation. Because of rapid variations in lateral stress with depth, probably as a result of localized influences and stratification, the data usually are not pooled or averaged but are reported separately.)

In Fig. 7 the data plot for the silt shows no elastic response and a high  $r^2$ , supporting the thesis that consolidation is occurring and is the main factor affecting the measured pressures. A limit pressure was reached on the fourth blade step. The soil was not saturated, and  $K_0$  was calculated to be about 1.5, indicative of overconsolidation. Since the loess at this site has no known history of preloading and contains montmorillonite, the lateral stresses may be attributable to clay expansion following an initial aeolian deposition.

Also in Fig. 7, the data for the sand show no clear indication of an elastic response or of a limit pressure and an acceptable  $r^2$ . The calculated value for  $K_0$  is about 0.8. As later will be shown, a graph of lateral stress versus depth in this sand indicates a slight overconsolidation.

It Fig. 8, the very stiff clay is a Vertisol, meaning that field evidence indicates it has expanded to the point of lateral pressure relief through shearing. Stepped blade measurements

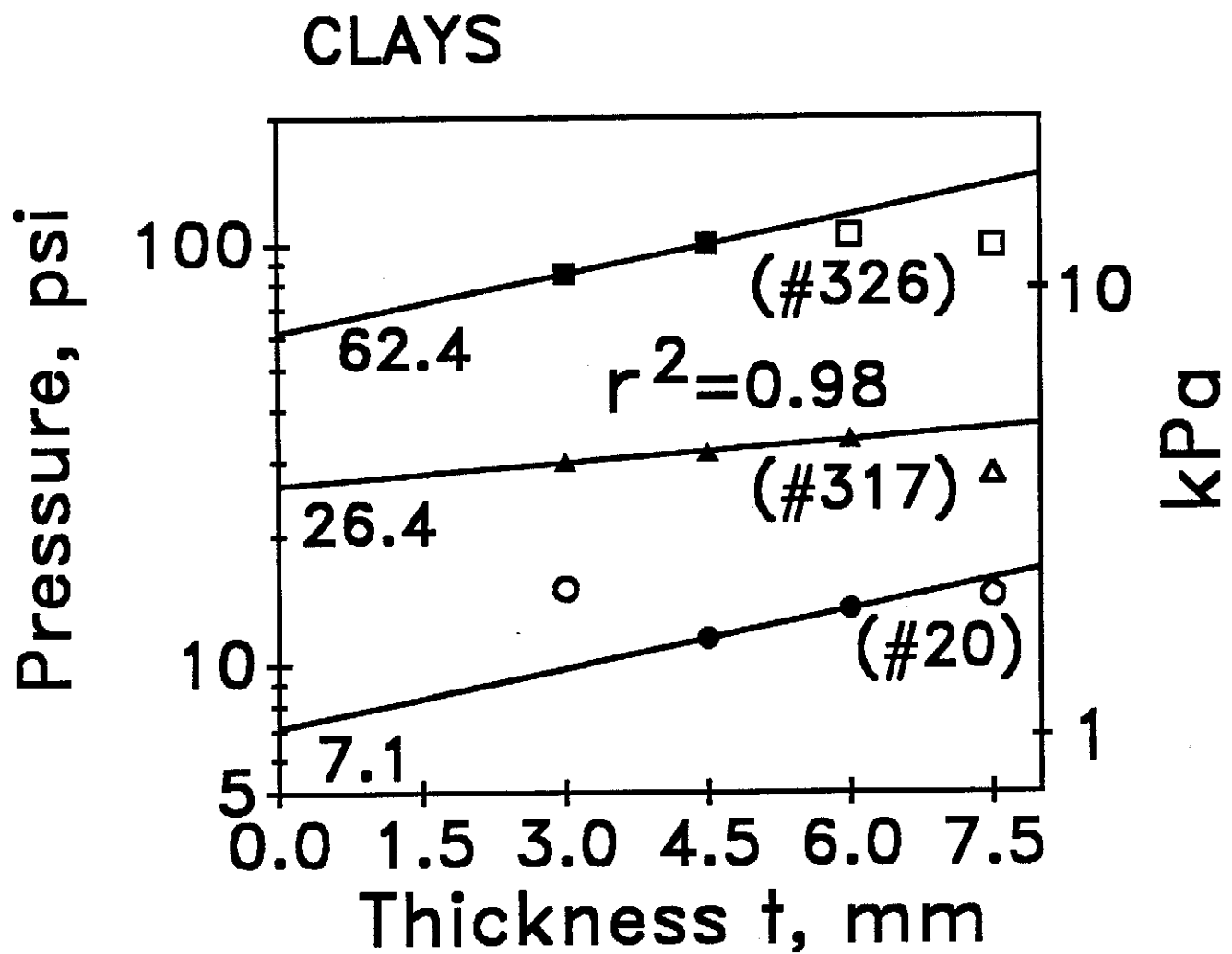


Fig. 8. Representative test data for some clays. Open points were not included in the regressions, representing either initial elastic response or limit pressure.

indicate that the lateral stress is quite high, giving  $K_0$  at this depth of about 4. The limit pressure also is high, and is several times higher than the unconfined compressive strength.

The medium clay in Fig. 8 also is a Vertisol, and blade tests at shallow depths at this site exactly duplicated lateral stresses obtained at the same site 6 years earlier with an older model blade (1, 6). At this depth,  $K_0$  is about 1.6. As in the case of the very stiff clay, the limit pressure is several times higher than the undrained shear strength reported by Mahar and O'Neill (8), probably because of the influence from confinement.

The soft clay test in Fig. 8 shows a breakdown of structure after penetration by the first step, making possible the determination of a subgrade modulus. The lateral stress is low for a soft clay, giving  $K_0$  of about 0.5, possibly indicative of underconsolidation which is consistent with the origin of this clay by recent sedimentation in an oxbow lake. The limit pressure approximates the calculated maximum for passive failure, discussed later in this paper.

These examples are included mainly to show representative test data and soil responses. For full interpretations of stress history of a soil, it is necessary to determine the relationships between lateral stress and depth, which is the subject of the remainder of this paper.

#### ILLUSTRATIONS OF USES OF THE $K_0$ STEPPED BLADE

##### Determination of the consolidation state

Overconsolidation. The stiff clays of Fig. 8 are determined to be overconsolidated, indicated by  $K_0 > 1$ , and attributable to



their expansive nature. In the sand of Fig. 9, the shaded area labeled "before pile driving" encloses a relatively narrow range of lateral stresses measured in this 50-year-old hydraulic fill sand. (The solid dot is the pressure extrapolated from sand data in Fig. 7.) A trend line through the data intersects the ground surface at a lateral pressure of about 3 psi (21 kPa); the corresponding vertical surcharge load may be obtained by extending the trend line upward to intersect the y axis, which occurs at an above-ground height of 10.9 ft (3.3 m), indicating prior existence of that amount of surcharge or its weight equivalent. The prior surcharge thus obtained is 0.66 Tsf, indicative of a moderate degree of overconsolidation that is as might be expected in an equipment storage yard. The slope of the trend line also allows an estimation of the friction angle from the Jaky equation; but because this estimate is based on lateral stresses developed as a consequence of consolidation, it probably contains no dilatant component. The angle so ascertained is  $20^{\circ}$ , which is considerably lower than the total-strength friction angle estimated at this site from cone and SPT tests (6). The sand is micaceous, which should contribute to low sliding friction.

Normal and underconsolidation. Fig.10 presents SBT data from the site of Jackson Lake Dam, Jackson Hole, Wyoming, after the dam had been removed due to a potential risk of liquefaction in this active earthquake area. The short-dashed line shows lateral stresses calculated assuming  $K_0 = 0.5$ , without the dam in place. It will be seen that below a depth of about 19 ft (6 m) the line approximately bisects the data, indicative that the soil there is normally consolidated if no consideration is given to

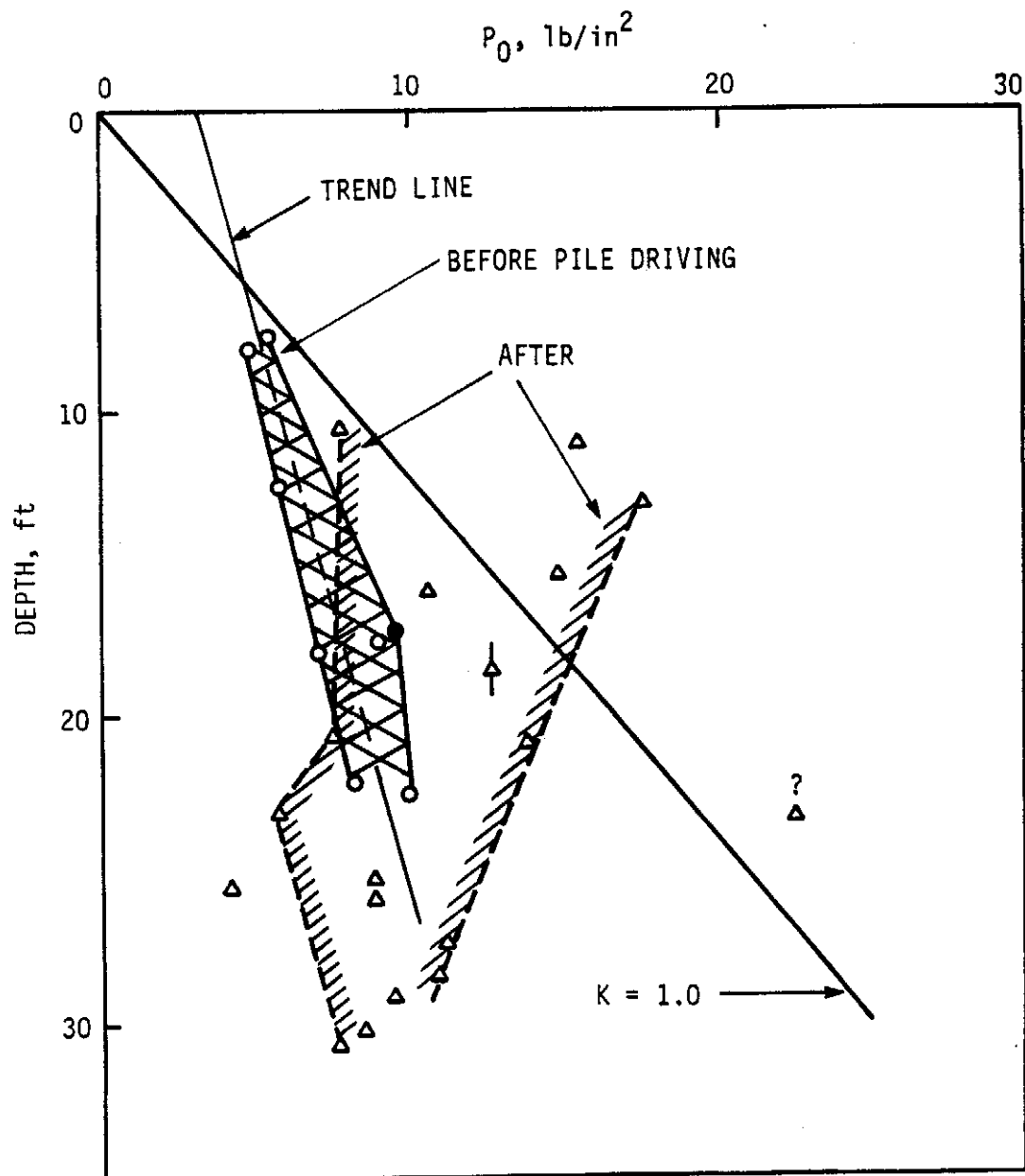


Fig. 9. Lateral stresses measured in a sand at Hunter's Point Naval Base, San Francisco. Note that  $K$  lines are calculated based on effective stress, then converted to total stress as measured by the Blade.

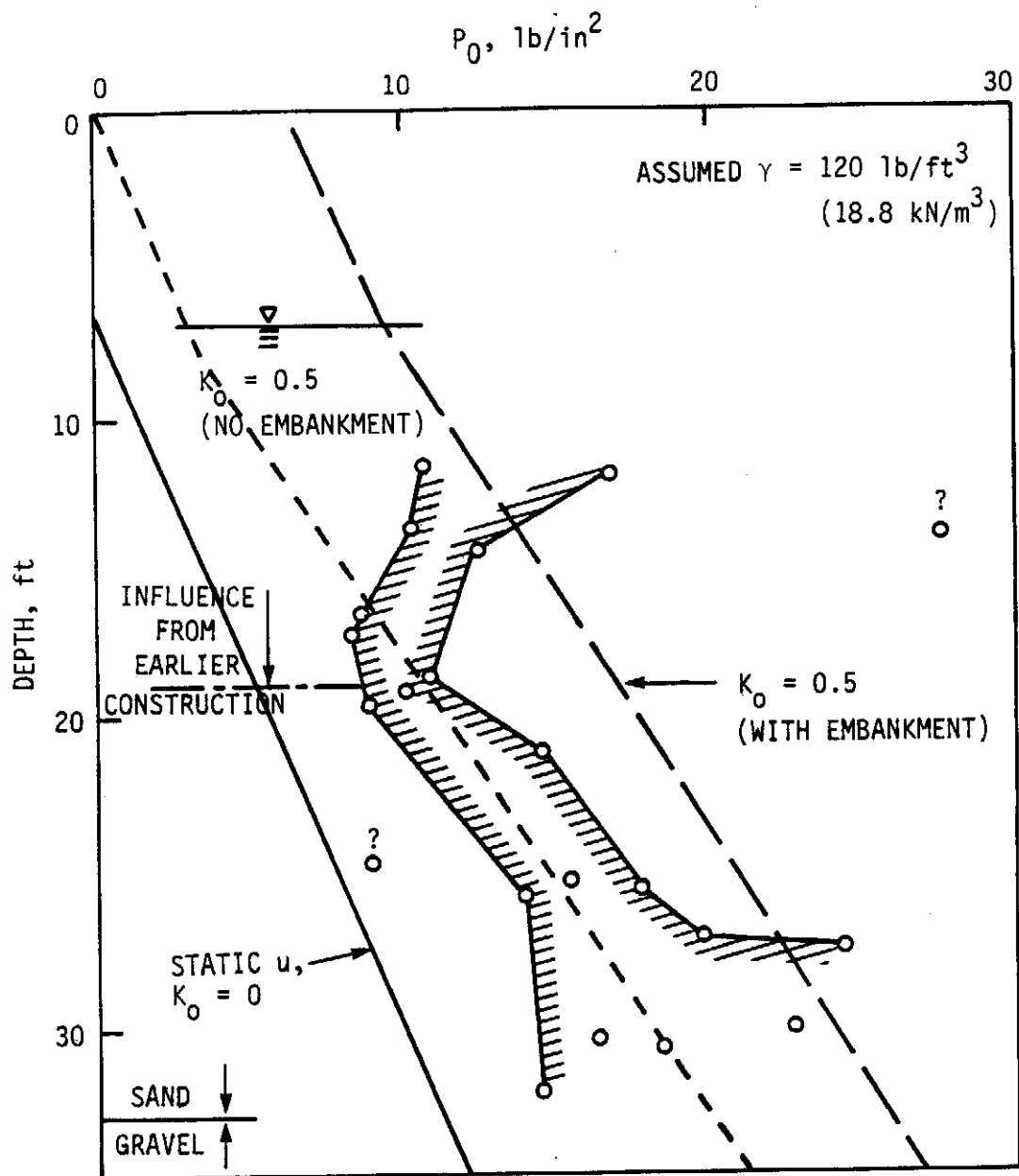


Fig. 10. Lateral stresses in sands and silts at Jackson Lake Dam, Wyoming, after removal of the dam and before dynamic compaction.

the weight of the dam. With the dam in place, soil below this depth would have been underconsolidated, which lends support to the thesis that the dam indeed was threatened by potential liquefaction of foundation soils, at least in the depth zone from 19 to 33 ft. At shallower depths the lateral stress data trend upward, approaching the  $K_0 = 0.5$  line that was calculated with consideration given to weight of the dam embankment. We therefore may conclude that at the shallower depths the soil was normally consolidated under the weight of the dam--and incidentally became overconsolidated when the dam was removed. Many other devices including the Menard pressuremeter, self-boring pressuremeter, and Dilatometer also were used at this site, with the latter giving the most closely comparable results.<sup>(12)</sup>

These examples illustrate of the use of lateral stress data to diagnose the soil consolidation state without the necessity for sampling and laboratory determination of a preconsolidation pressure, which is very sensitive to sample disturbance and is all but impossible to determine from laboratory tests of a sand. Such information can be vital. For example, recent tests made in relation to a metro tunneling project underneath an interstate highway gave an unexpected result that the silt soil that had been presumed to be residual and hence under high lateral stress from weathering expansion actually is normally consolidated, perhaps a colluvium, thus signaling that any additional load will cause appreciable settlement. In overconsolidated soils the inferred prior load obtained from lateral stress versus depth data may be an indication of how much surface load can be added

without appreciable settlement.

Detection of artificial compaction. Fig. 11 shows lateral stresses measured at the Jackson Dam site after dynamic compaction. Because the data were so erratic, an interpretation technique was used that involved determining average slopes "b" from the data plots, then applying that slope to individual points to increase the number of stress measurements (1). While this did not reduce the data scatter--in fact, it increased it--the additional points allowed a range of lateral stresses to be sufficiently well defined to suggest that the average  $K_0$  after compaction is about 1.0, which represents a substantial increase over the previous value of 0.5. The lateral stresses also are in the proper range for normal consolidation with the dam in place and  $K_0 = 0.5$ , which should move the soil into the safe range from liquefaction.

Fig. 12 shows data obtained in backfill soil that supposedly had been compacted some years previously behind a bridge abutment. As can be seen, most of the lateral stresses are far below the line for  $K_0 = 1$ , indicating that the soil had not been compacted. However, scattered high points, up to about 8 psi (60 kPa), occurred scattered throughout the height of the embankment. These random high stresses have the correct magnitude to have been caused from wheel contact pressures from earthmoving equipment during construction of the embankment.

Detection of grouting. While rather incidental to the studies at hand, one of the abutments of Fig. 12 gave some perplexingly high lateral stresses in the upper 11 ft (3.4 m) of

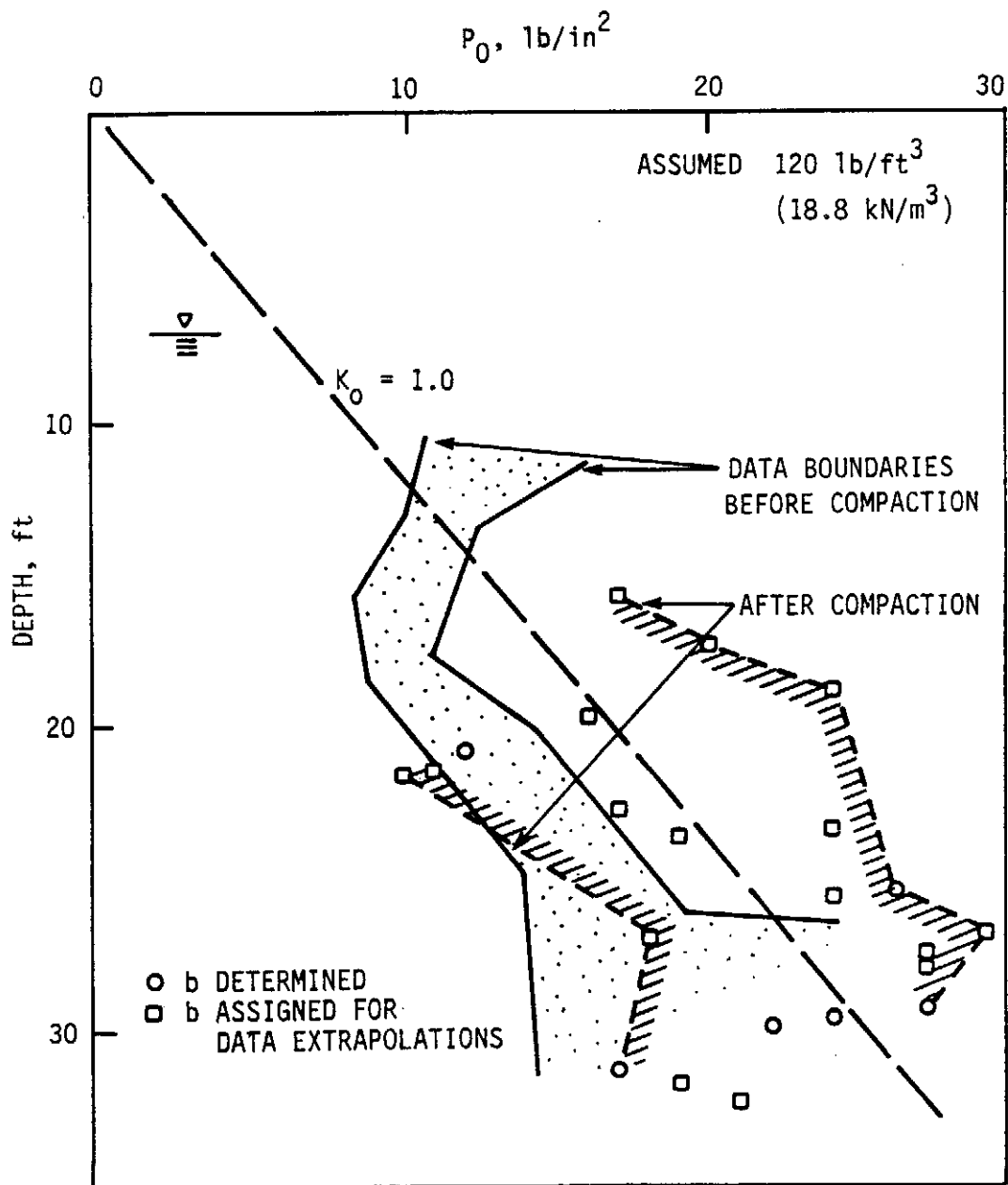


Fig. 11. Test results from the Jackson Lake site of Fig. 10 after deep dynamic compaction.

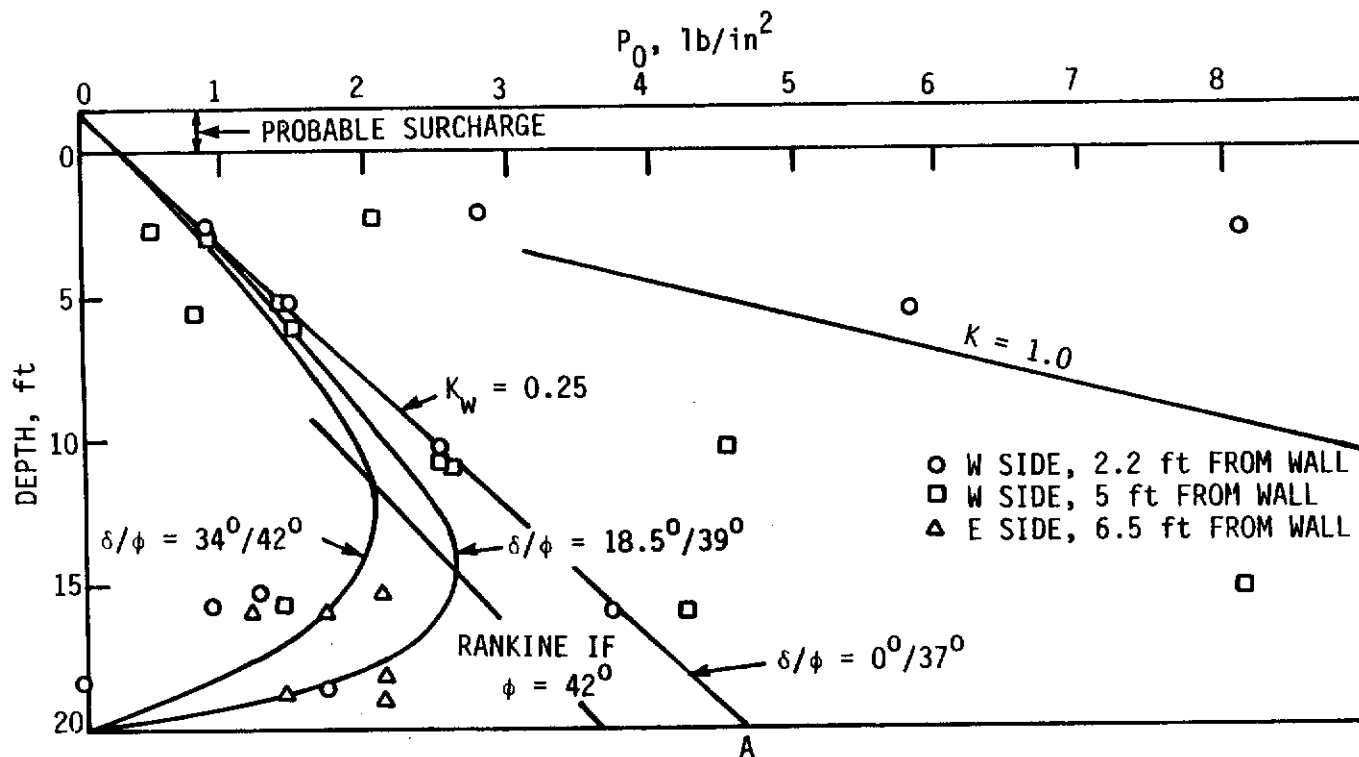


Fig. 12. Pressures against bridge abutments compared with predictions from Rankine and from a recent arching theory <sup>(10)</sup>. Data courtesy of Clyde Anderson, CTL/Thompson, Inc., Kellogg Engineering, Inc., and the City of Lakewood, Colo.

soil, as high as 24 psi (165 kPa), plotting far off of the graph to the right. It later was discovered that the soil had been pressure grouted in order to raise the approach slab. The average  $K_0$  in this zone is about 3, so pressures should have been high enough to do the job.

#### Detection of passive state pressures

Bearing capacity failure. Fig. 13 shows the distribution of lateral pressure with depth in a soft oxbow lake clay immediately lateral to a highway embankment then under construction. The tests were conducted before embankment construction and later when settlements became excessive and slope indicators showed lateral bulging outward of the foundation soil.<sup>(13)</sup> Lateral stresses were approximately twice what had been measured prior to the construction, and exceeded the theoretical maximum dictated by  $K_p$  calculated from before-construction borehole shear test data. The confluence of indicators suggested that it might be judicious for construction to be halted until pore pressures could dissipate, which was done. The embankment was completed the following construction season without incident.

Expansive clay. Tests for Fig. 12 were performed in soil that was known to be expansive, to determine if it was exerting undue pressure on adjacent bridge abutments. As can be seen from the data, this turned out not to be the case, as generally  $K_0 \ll 1$ . The bridge was removed without difficulty.

Fig. 14 shows lateral pressures versus depth in the very stiff expansive clay, including the data point from Fig. 8. The shaded zone includes three-fourths of the data points in a rela-



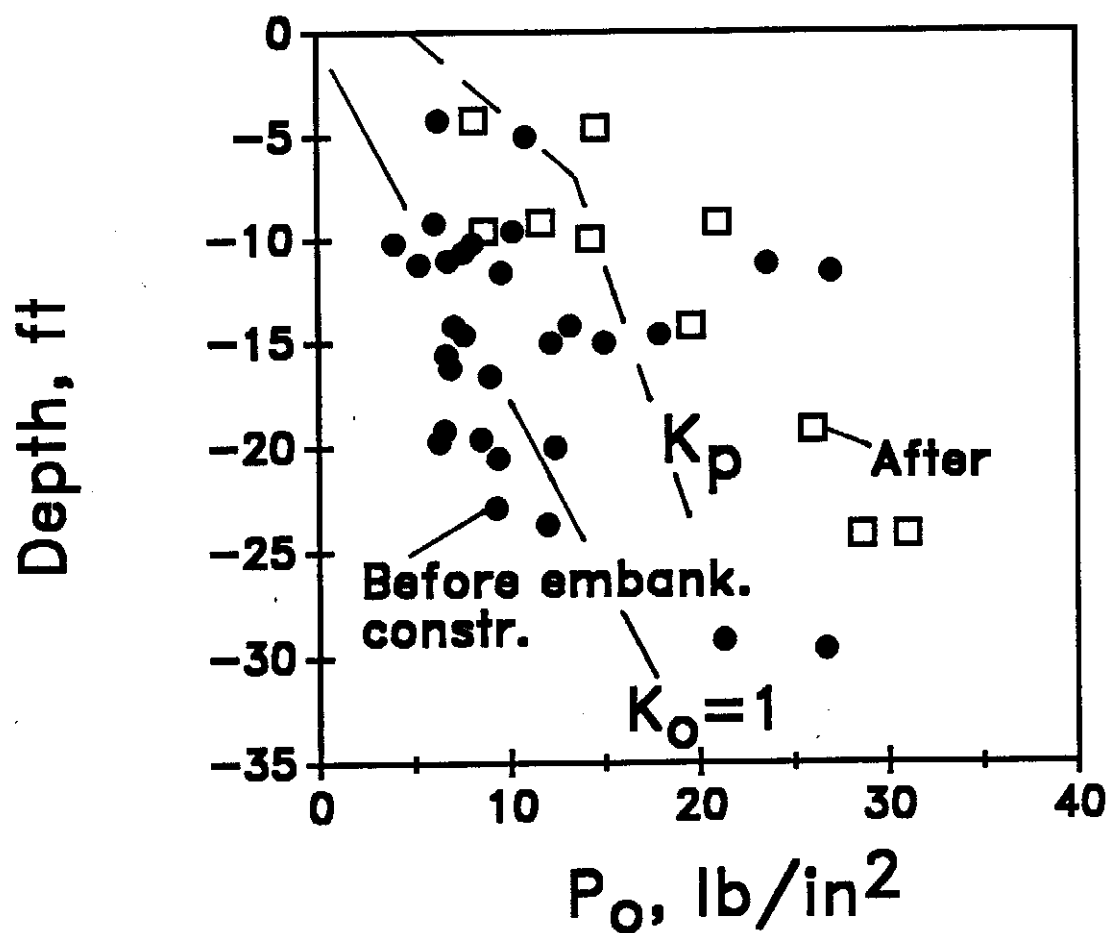


Fig. 13. Lateral stresses in a soft lakebed clay adjacent to a highway embankment, Storz Expressway, Omaha, Neb. Solid points are before embankment construction and open squares after, when there was concern for an impending bearing capacity failure.  $K_p$  line was drawn based on pre-construction shear tests.

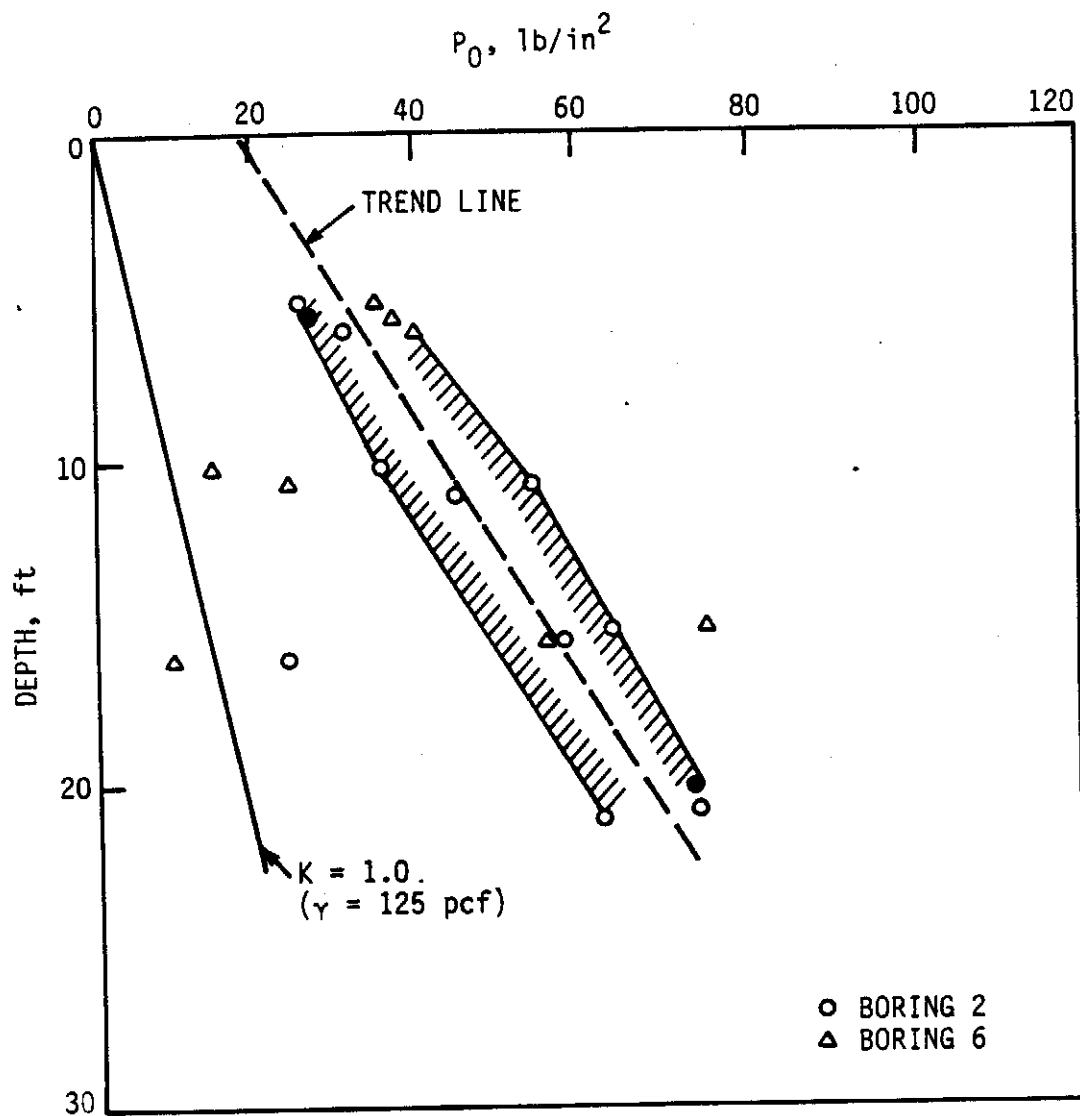


Fig. 14. Lateral stress data from a very stiff expansive clay, Texas A.&M. University, College Station, Texas.

tively narrow band. Since  $K_0 \gg 1$  and because this is a known Vertisol, passive conditions are suspected. To test this premise, two points were selected on the linear trend line for substitution of lateral and vertical stresses into the passive pressure equation, that then was solved simultaneously to give drained shear strength parameters. The equation is

$$\sigma_h = r z \tan^2(45 + \phi/2) + c \tan(45 + \phi/2) \quad (1)$$

Using this procedure with the data from Fig. 14, one obtains  $\phi = 28^\circ$  and  $c = 11.3$  psi (78 kPa). The equivalent unconfined compressive strength calculated from these values is 19 psi or 1.4 Tsf (131 kPa), which compares favorably with measured values that ranged from 0.8 to 1.6 Tsf, averaging about 1.2 Tsf (6, 9). This would appear to confirm that lateral stresses in this soil are being limited by passive failure. It also demonstrates how lateral stress data versus depth can be used to obtain meaningful representations for drained  $c$  and for  $\phi$  if the soil is in the passive state.

Slope stability. Unfortunately the potential for the blade test to measure passive pressures at the base of slopes and thus detect the potential for slope failure before movement occurs has not yet been realized, due to the difficulty of getting drilling machines into the toeslope areas. The potential is obvious, particularly in highway engineering, because it is simpler and cheaper to repair a slope before failure occurs than afterwards when the soil not only is in the wrong place, it has become permanently weakened through remolding and dilatancy drawing in more water. An indication of where pressures might appropriately be measured is shown in Fig. 15, after Dunlop and Duncan, who

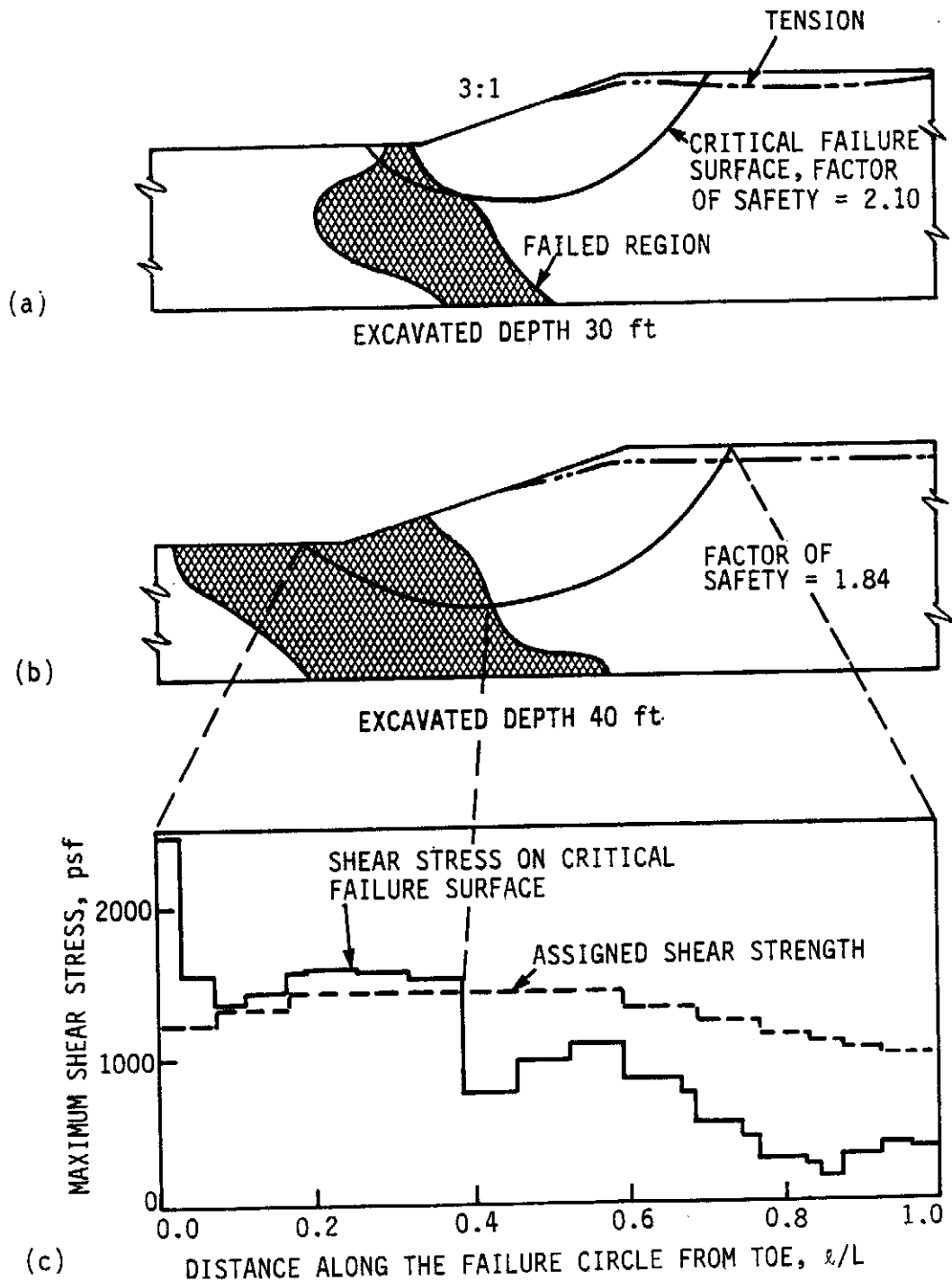


Fig. 15. Hypothetical failure zones from finite element analyses of a 3:1 slope excavated in overconsolidated clay, from Dunlop and Duncan (10).

based their study on finite element analyses (11). As can be seen, as simulated excavation proceeds, soil in the toe zone becomes stressed to its limit, which should initiate passive pressures. The extent to which passive pressures may develop without endangering a slope, and the relation to the existing factor of safety, are yet to be established.

#### Pressures adjacent to existing structures and driven pile

Fig. 12 shows lateral pressures measured in soil close to an existing wall, as already has been discussed. Fig. 9 shows the increase in shallow lateral soil stresses as the result of driving pile, and the disturbance to lateral soil pressures near the pile tip.

#### Subgrade modulus and limit pressure

An estimate for a lateral subgrade modulus  $k_b$  is obtained by dividing the pressure measured on the first blade step by one-half the blade thickness, or 1.5 mm. The value of the modulus depends in part on the size of area being loaded, and experience in the use of such  $k$  values is very limited and is not in the scope of this paper. An application of elastic theory to a blade area considered as a surface load gives the following relationship between  $k$  and the elastic modulus  $E$ :

$$E = 2.8 k \quad (2)$$

Application of this equation to the Houston clay data gives  $E$  values that are comparable to those obtained from UU triaxial tests, and lower by an order of magnitude than those obtained from cross-hole seismic studies (8). The modulus thus obtained from blade tests in a sand appeared to give an accurate predic-

tion of settlement of a bridge abutment (6).

### CONCLUSIONS

Development of a new apparatus requires a large investment of time, money, blind faith, and luck of the draw. Part of the attraction of a new tool is that it may open some doors that previously gave only a glimpse of future possibilities. Thus almost every test sequence has provided some surprises. For example, the commonly assumed lateral stresses characteristic of normal consolidation were found to be the exception instead of the rule, the actual stresses usually being higher, attributable to weathering expansion and clay expansion as well as to preloading. The ability to define the consolidation state in soils that cannot readily be sampled for laboratory tests, and to estimate the amount of the earlier surcharge from the pattern of lateral stress versus depth, can be expected to lend new intelligence to settlement studies. The determination of passive state pressures as invisible precursors for bearing capacity and slope failures may be of considerable utility for prescribing the ounce of prevention in lieu of the pound of cure.

### ACKNOWLEDGEMENTS

These studies were sponsored by the U.S. Federal Highway Administration under contract DTFG 61-84-000111, Carl Ealy the persevering contract manager. Data in Fig. 9 are used with the permission of Geo-Resource Consultants, Inc., San Francisco, courtesy of Eric Ng; in Fig. 10 and 11, with permission of Woodward-Clyde Consultants, Inc., Denver, courtesy of Dick Davidson; in Fig. 12, with permission of CTL-Thompson, Inc., Denver, the

tests having been performed by Clyde Anderson of that company; in Fig. 13, with permission of Woodward-Clyde Consultants, Inc., Omaha, courtesy of Steve Saye; in Fig. 14, courtesy of J.-L. Briaud and Texas A&M University. Many other companies and individuals also participated in these investigations, for which the authors extend their sincere gratitude.

#### REFERENCES CITED

1. Handy, R. L., Remmes, B., Moldt, S., and Lutenegeger, A. J., "In situ stress determination by Iowa Stepped Blade," ASCE Jour. of the Geotech. Engr. Div., Vol 108, Not GT11 (1982), pp. 1405-1422.
2. Handy, R. L., and Eichner, Don, "Back-pressured pneumatic pressure cell," U.S. Pat. No. 4,662,213 (1987).
3. Dunnicliff, John, Geotechnical instrumentation for monitoring field performance, New York: John Wiley & Sons (1988).
4. Lutenegeger, A. J., and Timian, D. A., "In situ tests with  $K_0$  Stepped Blade," ASCE Spec. Tech. Publ. No. 6 (1986), pp. 730-751.
5. Pabst, Mark, and Handy, R. L., "Soil effective stress sensor and method for using same," U.S. Pat. No. 4,524,626 (1985).
6. Handy, R. L., Briaud, J.-L., Gan, K. C., Mings, C. L., Retz, D. W., and Yang, J.-F., "Use of the  $K_0$  stepped blade in foundation design, Vol. I," Final Report, FHWA No. D-87/102 (June, 1987), NTIS, Springfield, Va. 22161.
7. Lutenegeger, A. J., personal communication.
8. Mahar, L. J., and O'Neill, M. W., "Field study of pile group action," FHWA No. RD-81/005 (1980).
9. Gan, K. C., "Evaluation of the stepped blade using the pressuremeter," unpubl. Ph.D. dissertation, Texas A&M University Library, College Station, Texas (1987)
10. Handy, R. L., "The arch in soil arching," ASCE Jour. of the Geotech. Engr. Div., Vol. 111, No. 3 (1985), pp. 302-308.
11. Dunlop, P., and Duncan, J. M., "Development of failure



around excavated slopes," ASCE Jour. of the Soil Mech. and Fd. Div., Vol 96, SM2 (1970), pp. 471-493.

12. Woodward-Clyde Consultants, Denver, Colo., "Assessment of in situ stress changes, Jackson Lake Dam, Minidoka Project, Jackson, Wyoming," Delivery Order No. 5, Contract No. 6-CA-30-02890, prepared for Bureau of Reclamation Embankment Dams Branch, Denver, Colo. (Sept., 1987)

13. Woodward-Clyde Consultants, Omaha, Nebr., "Analysis of instrumentation data, Arthur C. Storz Expressway, Omaha, Nebr." (August, 1989)

#### APPENDIX A

Flow chart for interpreting stepped blade pressure readings

1. First data point higher than second?.....Elastic response; do not include in extrapolation.
2. Last data points equal or lower than previous points, or plot low on the graph? .....Limit pressure; do not include in extrapolation.
3.  $r^2 < 0.97$  (where applicable).....Reexamine data for influence from possible limit pressure.
4. Line slope  $< 0.05 \text{ mm}^{-1}$ , possibly negative?.....All data probably exceed limit pressure; extrapolation not reliable..
5. 3 or 4 points with  $r^2 > 0.98$  and line slope  $> 0.05 \text{ mm}^{-1}$ ?.....Good test.